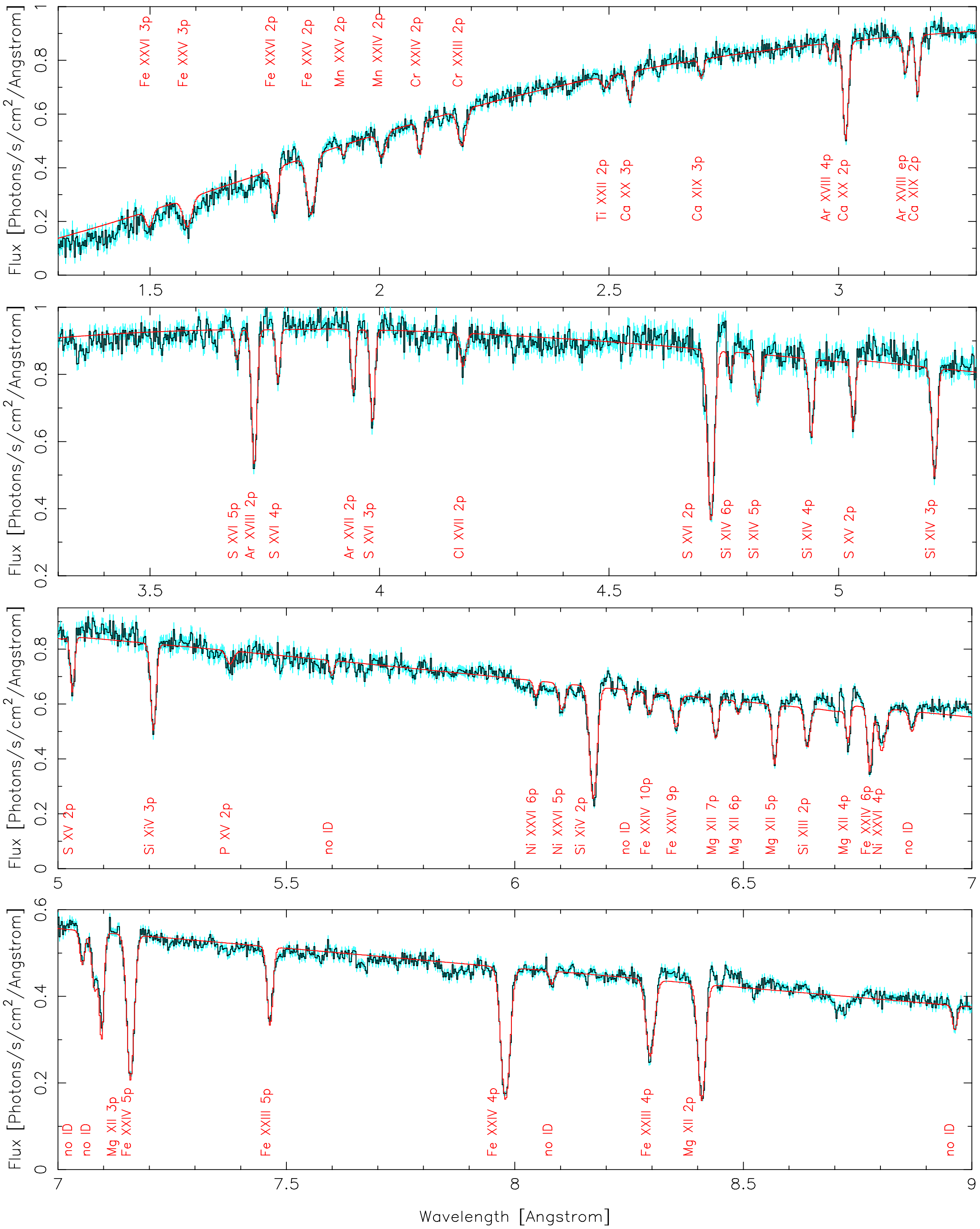

Supplementary Figure 1: The short wavelength portion of disk wind spectrum observed in the black hole GRO J1655−40 with Chandra. The data are shown in black, 1σ error bars are plotted in blue, and fits including local continuum models and Gaussian line functions are shown in red. Identifications for the lines are given in red. The parameters measured via this complex absorption spectrum are detailed in Supplementary Tables 1 and 2.

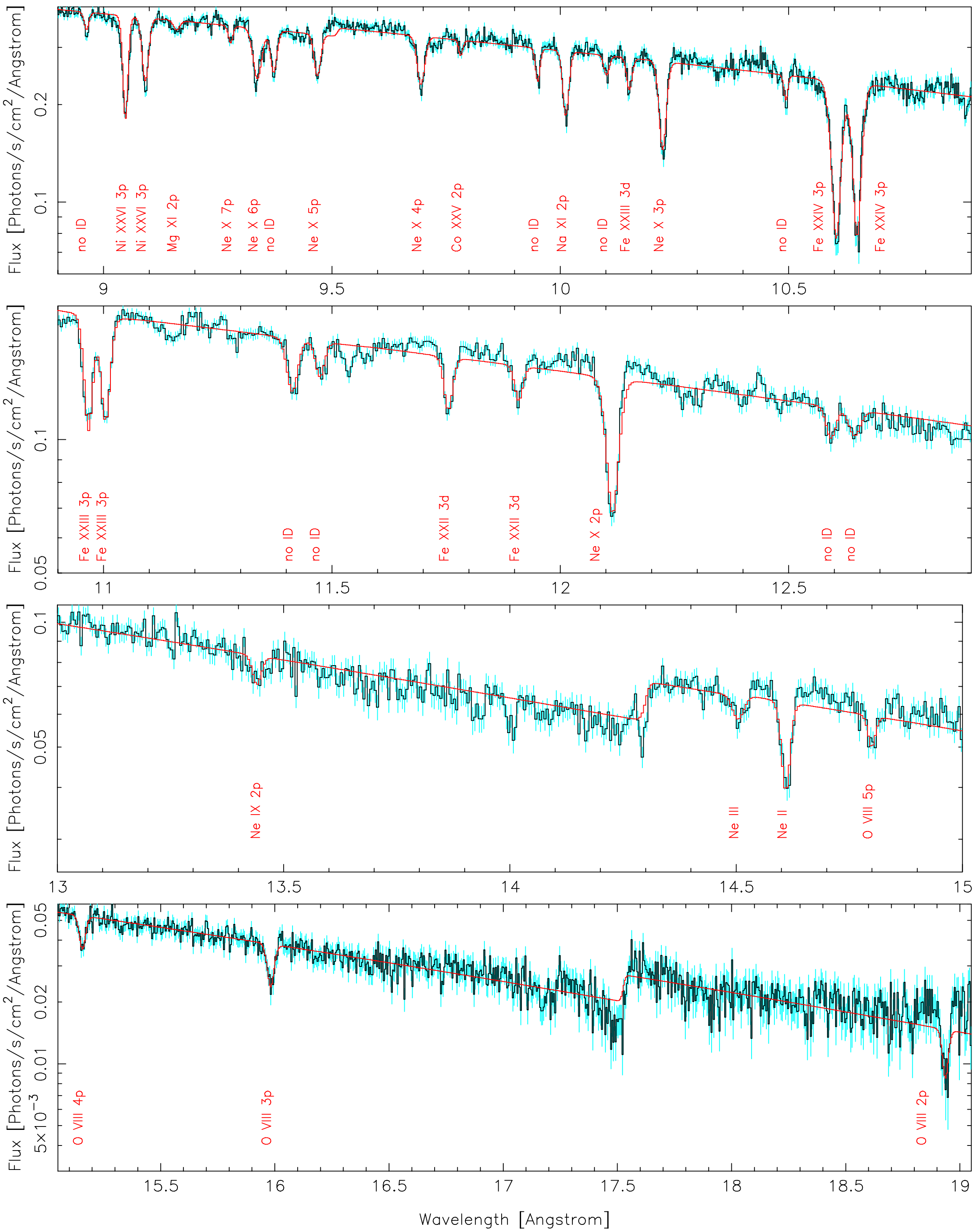

Supplementary Figure 2: The long wavelength portion of disk wind spectrum observed in the black hole GRO J1655−40 with Chandra. The data are shown in black, 1σ error bars are plotted in blue, and fits including local continuum models and Gaussian line functions are shown in red. Identifications for the lines are given in red. The parameters measured via this complex absorption spectrum are detailed in Supplementary Tables 1 and 2.

Ion and Transition	Meas. (Å)	Theor. (Å)	Shift (km/s)	FWHM (10^{-3}Å)	FWHM (km/s)	Flux (10^{-3} ph/cm^2/s)	W (mÅ)	N_Z (10^{17} cm^{-2})
O VIII $1s-5p$	14.800(2)	14.8206	420(40)	<10	<200	1.4(3)	23(5)	9(2)
O VIII $1s-4p$	15.157(2)	15.1762	380(40)	28(5)	550(80)	4.0(4)	77(8)	13(1)
O VIII $1s-3p$	15.982(2)	15.987	90(30)	31(5)	580(90)	5.1(5)	120(10)	7.5(8)
O VIII $1s-2p$	18.938(2)	18.9689	480(40)	24(5)	380(80)	1.2(2)	80(8)	0.7(1)
Ne X $1s-7p$	9.2786(6)	9.2912	410(20)	5(2)	200(100)	1.3(2)	3.6(7)	10(2)
Ne X $1s-6p$	9.3365(6)	9.3616	800(20)	22(1)	700(40)	6.6(3)	22(1)	35(1)
Ne X $1s-5p$	9.4685(4)	9.4807	390(20)	14(1)	440(30)	4.1(3)	12(1)	11(1)
Ne X $1s-4p$	9.6949(5)	9.7082	410(10)	18(2)	560(50)	5.5(3)	16(1)	6.6(3)
Ne X $1s-3p$	10.2246(3)	10.2389	420(10)	17(1)	500(30)	8.3(2)	30(7)	4.1(1)
Ne X $1s-2p$	12.1152(5)	12.1330	550(10)	29(1)	720(20)	8.2(4)	57(3)	1.05(5)
Ne IX $1s^2-1s2p$	13.441(4)	13.4471	140(80)	14	300	1.8(4)	22(5)	0.20(5)
Ne III	14.504(3)	14.526	450(50)	20(10)	400(200)	1.5(2)	22(3)	1.1(2)
Ne II	14.611(1)	14.631	410(20)	14(2)	300(30)	3.8(3)	58(5)	4.9(4)
Na XI $1s-2p$	10.0122(3)	10.0250	380(10)	13.2(5)	400(20)	5.6(2)	18.7(7)	0.51(2)
Mg XII $1s-7p$	6.4395(3)	6.4486	420(10)	9(1)	420(50)	3.2(1)	5.1(2)	28(1)
Mg XII $1s-6p$	6.4888(5)	6.4974	400(20)	<6	<300	0.8(1)	1.3(2)	4.4(6)
Mg XII $1s-5p$	6.5685(2)	6.5801	530(10)	8.0(5)	360(30)	4.7(1)	7.7(2)	14.4(4)
Mg XII $1s-4p$	6.7275(3)	6.7379	460(10)	<6	<300	2.5(1)	4.2(2)	3.6(2)
Mg XII $1s-3p$	7.0969(4)	7.1062	390(20)	5.4(5)	230(20)	3.9(3)	9.8(9)	2.8(3)
Mg XII $1s-2p$	8.4087(2)	8.4210	440(10)	16.7(3)	590(10)	9.6(1)	22.6(2)	0.87(1)
Mg XI $1s^2-1s2p$	9.159(2)	9.1688	320(70)	13	400	1.0(1)	2.7(3)	0.049(5)
Si XIV $1s-6p$	4.764(2)	4.7704	400(100)	<5.0	<300	1.0(1)	1.2(1)	7.5(8)
Si XIV $1s-5p$	4.8243(7)	4.8311	420(40)	9(2)	600(100)	2.4(2)	2.8(2)	9.7(9)
Si XIV $1s-4p$	4.9407(3)	4.9469	380(20)	6(1)	360(60)	3.6(2)	4.2(2)	6.7(3)
Si XIV $1s-3p$	5.2090(3)	5.2172	470(20)	9.7(7)	560(40)	5.9(2)	7.2(2)	3.8(1)
Si XIV $1s-2p$	6.1721(1)	6.1822	490(10)	15.5(2)	750(10)	11.9(1)	18.5(2)	1.32(1)
Si XIII $1s^2-1s2p$	6.6402(2)	6.6480	350(10)	10(1)	450(50)	3.4(1)	5.7(1)	0.19(1)
P XV $1s-2p$	5.375(2)	5.383	700(200)	–	400	1.0(2)	1.3(3)	0.12(3)
S XVI $1s-5p$	3.690(1)	3.6959	480(80)	<5	<400	1.1(2)	1.2(2)	7(1)
S XVI $1s-4p$	3.780(1)	3.7845	360(80)	<5	<400	1.9(2)	2.0(2)	5.4(5)
S XVI $1s-3p$	3.9858(3)	3.9912	400(30)	6(1)	450(80)	3.9(2)	4.2(2)	3.8(2)
S XVI $1s-2p$	4.7221(2)	4.7292	450(10)	14.4(7)	910(50)	11.3(2)	12.8(2)	1.55(2)
S XV $1s^2-1s2p$	5.0318(4)	5.0387	410(20)	<5	<400	2.9(2)	3.4(2)	0.20(2)

Supplementary Table 1: Parameters of the disk wind absorption lines observed in GRO J1655−40 for elements with $Z < 17$. For clarity, the lines are listed by element in order of ascending atomic number, and in order of increasing wavelength by element and ion. The spectral continua were fit locally using power-law models modified by neutral photoelectric absorption edges (due to the interstellar medium) where appropriate. The lines were fit with simple Gaussian models. The errors quoted above are 1σ uncertainties. Line significances were calculated by dividing line flux by its 1σ error. Where errors are not given, the parameter was fixed at the quoted value. Line widths consisent with zero are not resolved.

Ion and Transition	Meas. (Å)	Theor. (Å)	Shift (km/s)	FWHM (10^{-3} Å)	FWHM (km/s)	Flux (10^{-3} ph/cm^2/s)	W (mÅ)	N_Z (10^{17} cm^{-2})
Cl XVII $1s-2p$	4.182(1)	4.187	400(100)	9(2)	600(200)	1.5(2)	1.6(2)	0.25(3)
Ar XVIII $1s-4p$	2.981(1)	2.9875	700(100)	<5	<500	0.8(1)	0.9(1)	3.9(5)
Ar XVIII $1s-3p$	3.1454(5)	3.1506	500(50)	6(1)	600(100)	2.0(2)	2.2(2)	3.2(3)
Ar XVIII $1s-2p$	3.7271(2)	3.7329	470(20)	8.7(7)	700(50)	6.3(2)	8.0(3)	1.6(1)
Ar XVII $1s^2-1s2p$	3.9429(4)	3.9488	450(30)	<5	<500	2.3(1)	2.6(1)	0.24(1)
K XIX $1s-2p$	–	3.348	–	–	800	1.0(2)	1.0(2)	0.24(5)
Ca XX $1s-3p$	2.5452(6)	2.5494	490(70)	9(2)	1100(100)	1.7(2)	2.2(2)	4.8(5)
Ca XX $1s-2p$	3.0187(2)	3.0203	160(20)	9.2(7)	910(70)	5.75(7)	6.66(8)	2.0(1)
Ca XIX $1s^2-1s3p$	2.701(1)	2.7054	500(100)	<10	<1100	0.9(1)	1.1(1)	1.1(1)
Ca XIX $1s^2-1s2p$	3.1722(3)	3.1772	470(30)	<10	<1100	2.9(2)	3.2(2)	0.46(4)
Sc XXI $1s-2p$	–	2.740	–	–	1500	<0.1	<0.13	<0.05
Ti XXII $1s-2p$	2.493(2)	2.4966	430(240)	17(5)	2000(600)	1.0(2)	1.3(3)	1.7(3)
V XXIII $1s-2p$	–	2.2794	–	–	1500	<0.7	<0.7	<0.4
Cr XXIV $1s-2p$	2.0880(6)	2.0901	300(80)	10(2)	1400(300)	2.0(2)	3.4(3)	6.3(6)
Cr XXIII $1s^2-1s2p$	2.1794(6)	2.1821	370(80)	19(2)	2600(300)	3.1(2)	4.8(3)	1.6(2)
Mn XXV $1s-2p$	1.922(2)	1.9247	400(300)	<154	<2000	0.5(1)	1.0(2)	1.1(2)
Mn XXIV$1s^2-1s2p$	2.005(1)	2.0062	200(140)	17(2)	2500(300)	2.0(2)	3.7(4)	3.7(4)
Fe XXVI $1s-3p$	1.498(2)	1.5028	1000(400)	12	2400	1.1(2)	5(1)	32(6)
Fe XXVI $1s-2p$	1.7714(5)	1.7798	1400(100)	12(1)	2400(200)	3.1(2)	7.8(5)	6.7(4)
Fe XXV $1s^2-1s3p$	1.581(1)	1.5732	1500(200)	20	3800	2.6(2)	9.7(9)	28(3)
Fe XXV $1s^2-1s2p$	1.8510(4)	1.8504	0(100)	20(1)	3800(300)	5.4(2)	12.6(5)	5.2(2)
Fe XXIV $1s^22s-1s^210p$	6.2946(5)	6.3055	–	10(1)	480(40)	1.8(2)	2.8(3)	21(1)
Fe XXIV $1s^22s-1s^29p$	6.3523(4)	6.3475	–	14(1)	660(50)	3.3(2)	5.2(3)	28(2)
Fe XXIV $1s^22s-1s^28p$	blend	–	–	–	–	–	–	–
Fe XXIV $1s^22s-1s^27p$	blend	–	–	–	–	–	–	–
Fe XXIV $1s^22s-1s^26p$	6.7773(2)	6.7870	430(10)	8.2(5)	360(20)	5.4(1)	10.2(2)	11.9(2)
Fe XXIV $1s^22s-1s^25p$	7.1590(1)	7.1690	420(10)	15.8(2)	660(10)	10.37(3)	19.3(1)	10.6(1)
Fe XXIV $1s^22s-1s^24p$	7.9795(1)	7.9893	370(10)	20.2(1)	760(10)	13.1(2)	28.2(4)	5.15(7)
Fe XXIV $1s^22s-1s^23p$	10.6043(3)	10.619	420(10)	27.3(7)	770(20)	13.7(4)	60(1)	2.30(4)
Fe XXIV $1s^22s-1s^23p$	10.6494(3)	10.663	380(10)	23.8(5)	670(20)	11.9(2)	52(1)	3.95(5)
Fe XXIII $2s^2-2s5p$	7.4639(2)	7.4722	330(10)	11.6(5)	470(20)	4.15(4)	8.2(1)	2.27(4)
Fe XXIII $2s^2-2s4p$	8.2963(2)	8.3029	240(10)	18.1(5)	650(20)	7.0(1)	16.3(2)	1.49(2)
Fe XXIII $2s^2-2p3d$	10.1512(6)	10.175	700(20)	10(2)	290(60)	2.7(2)	16(2)	5.3(7)
Fe XXIII $2s^2-2p3s$	–	10.560	–	–	–	–	–	–
Fe XXIII $2s^2-2s3p$	10.9671(3)	10.981	380(10)	16(1)	440(30)	7.0(3)	40(2)	0.54(3)
Fe XXIII $2s^2-2s3p4$	11.0049(5)	11.018	360(10)	17(1)	460(30)	6.8(3)	33(2)	1.1(1)
Fe XXII $2s^22p-2s^23d$	11.755(1)	11.770	380(20)	14(2)	360(50)	2.4(3)	14(2)	0.17(2)
Fe XXII $2s^22p-2s^23d$	11.909(2)	11.920	280(50)	10(2)	250(50)	1.8(3)	11(2)	0.15(2)
Ni XXVI $1s^22s-1s^26p$	6.045(1)	–	–	9.2(5)	450(30)	1.4(2)	2.1(3) –	
Ni XXVI $1s^22s-1s^25p$	6.103(1)	6.120	830(50)	16(2)	800(100)	2.6(2)	3.9(4)	4.2(5)
Ni XXVI $1s^22s-1s^24p$	6.8029(4)	6.8163	650(20)	27(1)	1200(50)	5.7(1)	9.5(2)	2.3(1)
Ni XXVI $1s^22s-1s^23p$	9.0479(2)	9.061	430(10)	15.1(5)	500(20)	6.6(1)	18.5(3)	1.04(1)
Ni XXVI $1s^22s-1s^23p$	9.0917(4)	9.105	440(10)	11.8(4)	400(30)	4.5(1)	12.4(3)	1.31(3)
Co XXV $1s^22s-1s^23p$	9.782(1)	9.795	400(40)	8(4)	200(100)	1.0(2)	3.2(6)	0.15(3)
no ID; Al XIII $1s-5p$?	5.600(1)	–	–	6(2)	400	0.85(15)	1.1(2)	–
no ID; Ni XXVI $2p-5d$?	6.250(1)	–	–	<4	<200	1.0(2)	1.5(3)	–
no ID; Ni XXVI $2p-4s$?	7.0555(8)	–	–	7(2)	300(100)	1.3(1)	2.4(2)	–
no ID; Ni XXVI $2p-4d$?	7.0815(8)	–	–	12(2)	500(100)	3.0(3)	5.4(5)	–
no ID; Ni XXVI $2p-3d$?	9.3726(4)	–	–	14(1)	450(30)	4.2(2)	12.3(6)	–
no ID; Ni XXV $2s2p-2s3d$?	9.9509(5)	–	–	6(2)	200(50)	2.3(2)	7.7(6)	–
no ID	6.8690(5)	–	–	10(2)	440(80)	1.7(1)	2.9	–
no ID	8.081(2)	–	–	7(2)	260(80)	0.6(1)	1.4	–
no ID	8.960(1)	–	–	<5	<200	1.0(1)	2.6	–
no ID	10.1015(6)	–	–	12(5)	400(100)	1.7(2)	5.8	–
no ID	10.494(1)	–	–	3(3)	100(100)	1.5(2)	6.2	–
no ID	11.413(2)	–	–	57(9)	1500(200)	7(1)	38.9	–
no ID	11.472(2)	–	–	12(5)	300(100)	1.6(3)	10.7	–
no ID	12.593(2)	–	–	19(7)	500(200)	2.3(4)	19.5	–
no ID	12.644(3)	–	–	24(7)	600(100)	2.1(4)	18.7	–

Supplementary Table 1: Parameters of the disk wind absorption lines observed in GRO J1655−40 for elements with $Z \geq 17$. For clarity, the lines are listed by element in order of ascending atomic number, and in order of increasing wavelength by element and ion. The spectral continua were fit locally using power-law models modified by neutral photoelectric absorption edges (due to the interstellar medium) where appropriate. The lines were fit with simple Gaussian models. The errors quoted above are 1σ uncertainties. Line significances were calculated by dividing line flux by its 1σ error. Where errors are not given, the parameter was fixed at the quoted value. Line widths consisent with zero are not resolved.